

Time dependence of Poisson's effect in wood III: asymmetry of three-dimensional viscoelastic compliance matrix of Japanese cypress

Kosei Ando · Mayu Mizutani · Yusuke Taniguchi ·
Hiroyuki Yamamoto

Received: 24 December 2012 / Accepted: 13 February 2013 / Published online: 28 February 2013
© The Japan Wood Research Society 2013

Abstract To understand the viscoelasticity of wood three dimensionally, matched samples of Japanese cypress were loaded in uniaxial tensile creep in the longitudinal (L), radial (R), and tangential (T) directions at approximately 9.7 % equilibrium moisture content. Longitudinal and transverse strains were measured for the determination of viscoelastic Poisson's ratios and three-dimensional viscoelastic compliance tensors concerning the normal strain. The changes in the transverse strains showed the same tendencies as those in the longitudinal strains, in all directions of loading. That is, during creep, the absolute value of transverse strain continued to increase with the gradual reduction in the increase rate; immediately after the removal of the load, it recovered rapidly, after which it continued to recover slowly. The transverse strain increased most easily in the T direction, followed by R and L, during creep. All the viscoelastic Poisson's ratios and the absolute values of all elements of the viscoelastic compliance increased logarithmically with creep time. The three-dimensional viscoelastic compliance matrix for Japanese cypress is concluded to be asymmetric.

Keywords Viscoelasticity · Normal strain · Creep compliance · Transverse strain · Poisson's ratio

Preliminary report of this study was published in this journal, 56: 82–84 (2010).

K. Ando (✉) · M. Mizutani · H. Yamamoto
Graduate School of Bioagricultural Sciences,
Nagoya University, Chikusa-ku, Nagoya 464-8601, Japan
e-mail: musica@agr.nagoya-u.ac.jp

Y. Taniguchi
Building Products Headquarters, Daiken Corporation,
3-12-8 Sotokanda, Chiyoda-ku, Tokyo 101-8950, Japan

Introduction

Two of the unique characteristics of wood as a material are its orthotropy and its viscoelasticity. Therefore, it will be essential to formulate two- or three-dimensional viscoelastic functions that can be employed for rigorous stress–strain analyses for wood to make wider use of this material in designs involving combined stress in the future. A one-dimensional theory of the viscoelasticity for wood has almost been established with a few exceptions, e.g., behavior in a non-equilibrium moisture state and behavior under shear stress. Nonetheless, as of this writing, there has yet to be almost any research, either theoretical or experimental, toward establishing a two- or three-dimensional viscoelastic theory for wood.

Poisson's ratio is one of the elastic constants for describing the stress–strain relationship in an elastic body in two dimensions. When a material is subjected to tension, it shrinks in the transverse direction (perpendicular to the direction of the force). Conversely, when it is compressed, it swells in the transverse direction. This behavior is called the Poisson effect. Poisson's ratio (ν_{ij}) is expressed as follows:

$$\nu_{ij} = -\frac{\varepsilon_j}{\varepsilon_i} \quad (i, j = L, T, R) \quad (1)$$

where ε_i is the longitudinal (positive) strain in the loading direction and ε_j is the transverse (passive) strain in the perpendicular direction; the subscripts i and j index the three orthogonal directions in wood, i.e., longitudinal (L), radial (R), and tangential (T) directions. Non-contact strain measurement technologies based on image analysis have made some contributions to research into Poisson's ratio in the orthotropic material wood, and this is currently a quite popular topic of research. Within the research on Poisson's

ratio, a large variety of sub-topics exists: earlywood or latewood [1–3]; in-plane distribution [4, 5]; the relationships with the microstructure of the cell wall [6–9]; the influences of moisture content [10, 11], grain angle [12], annual ring angle [13], and loading rate [14, 15]; compressed or heat-treated wood [16–18]; and Poisson’s ratios in the three orthogonal planes (LR, LT, and RT planes) in wood [14, 19, 20]. Sliker et al. [14] have measured Poisson’s ratios and Young’s moduli in 10 species of hardwoods to determine all elastic compliance tensors concerning the normal strain.

Since Poisson’s ratio is an elastic constant, it cannot vary with time. Nevertheless, it has been theoretically proven that the Poisson effect in viscoelastic materials,

whether isotropic or orthotropic, is time dependent [21, 22]. The apparent Poisson’s ratio is therefore referred to as the viscoelastic Poisson’s ratio, which is defined as follows:

$$v_{ij}(t) = -\frac{\epsilon_j(t)}{\epsilon_i(t)} \quad (i, j = L, T, R) \quad (2)$$

An introduction of the concept of the viscoelastic Poisson’s ratio to viscoelasticity should provide clues on how to expand the one-dimensional law of viscoelasticity to two or three dimensions in a way analogous to the generalization of Hooke’s law in elasticity [23]. Some reports concerning the viscoelastic Poisson’s ratio are available to resolve the two-dimensional viscoelasticity of

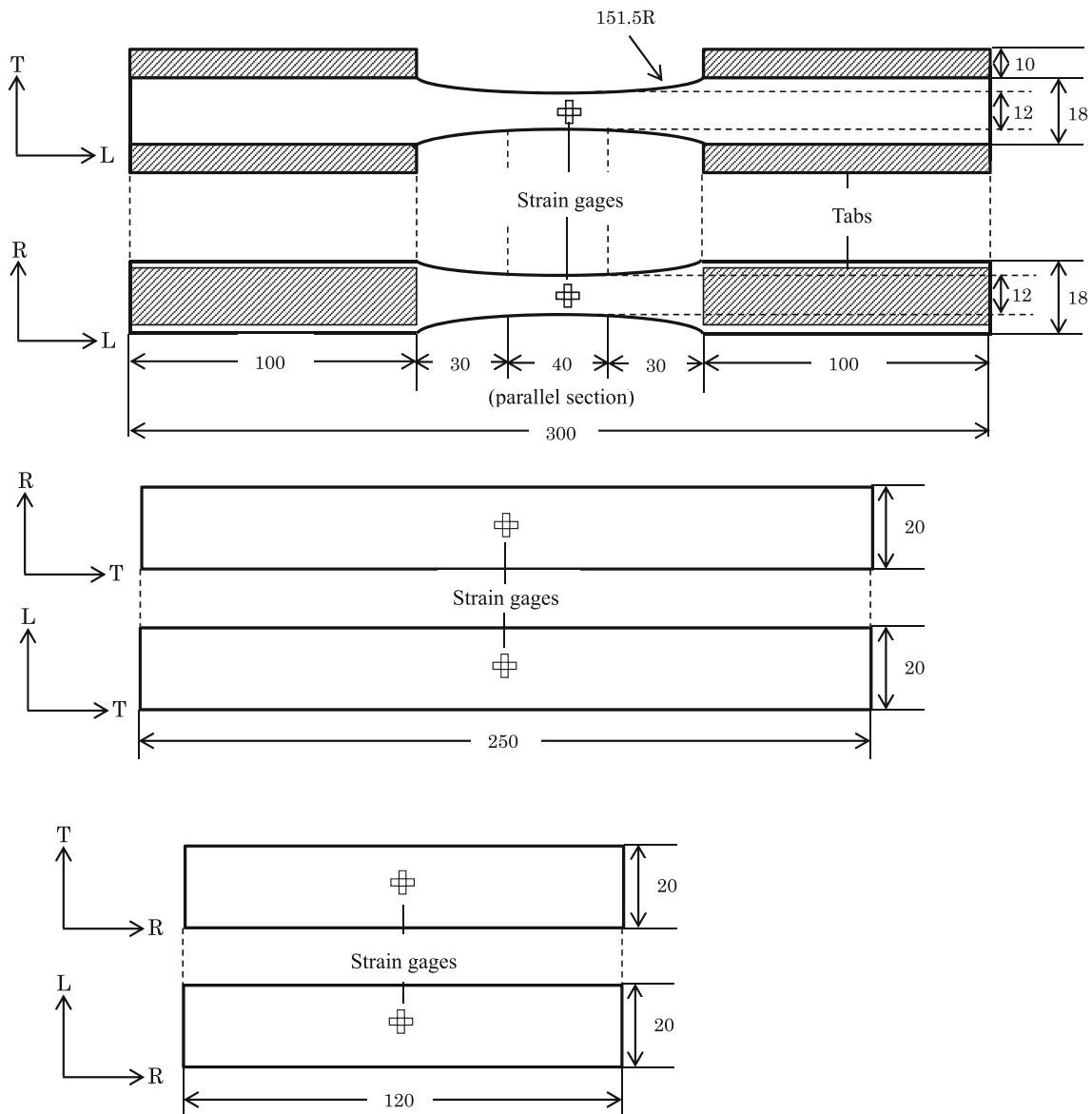


Fig. 1 Tensile test specimens. A biaxial strain gauge was pasted on each of the four planes. Unit: mm. *Upper* L-specimen, *middle* T-specimen, *lower* R-specimen

wood. Schniewind et al. [24] measured $v_{LR}(t)$, $v_{LT}(t)$, and $v_{TL}(t)$ in Douglas-fir by conducting tensile creep tests; they reported that all three decreased with time and that they had found no remarkable asymmetry in the two-dimensional viscoelastic compliance matrix for the LT plane. Sobue et al. [23] measured $v_{LR}(t)$ and $v_{RL}(t)$ in Japanese cypress, Japanese beech, and Japanese zelkova by the method of free-free beam vibration, and found that the two-dimensional viscoelastic stiffness matrix was asymmetric, which contradicted the results of Schniewind et al. Hayashi et al. [25] measured $v_{LR}(t)$ in Norway spruce by tensile creep tests and observed that the change in $v_{LR}(t)$ during creep was quite small; they implied that $v_{LR}(t)$ could be considered to be equal to Poisson's ratio, in other words $v_{LR}(t = 0)$. Taniguchi et al. [26] measured $v_{LR}(t)$ and $v_{LT}(t)$ in wood of 12 species by tensile creep tests and reported that the viscoelastic Poisson's ratios increased with time, contradicting the results of Schniewind et al.; Taniguchi et al. also stated that the

reason for the increase in viscoelastic Poisson's ratios was a remarkable enlargement of the permanent transverse strain, which they attributed to the occurrence or growth of microcracks. Furthermore, they reported that the volume of wood decreased due to the Poisson effect during both creep and creep recovery, which would be a unique property of wood as a material [27]. Although Schniewind et al. and Sobue et al. have measured the viscoelastic compliance in two dimensions, there has been almost no research into the three-dimensional viscoelastic compliance of woods, in spite of the fact that wood has three axes of symmetry.

The purpose of the present study is to extend the previous biaxial, two-dimensional approach for determining the viscoelastic functions for wood to three dimensions. Uniaxial creep tests were performed on Japanese cypress in the L, T, and R directions, and the longitudinal and transverse strains were observed during creep and creep recovery. All components of the three-dimensional viscoelastic compliance tensor concerning the normal strain were determined. Most

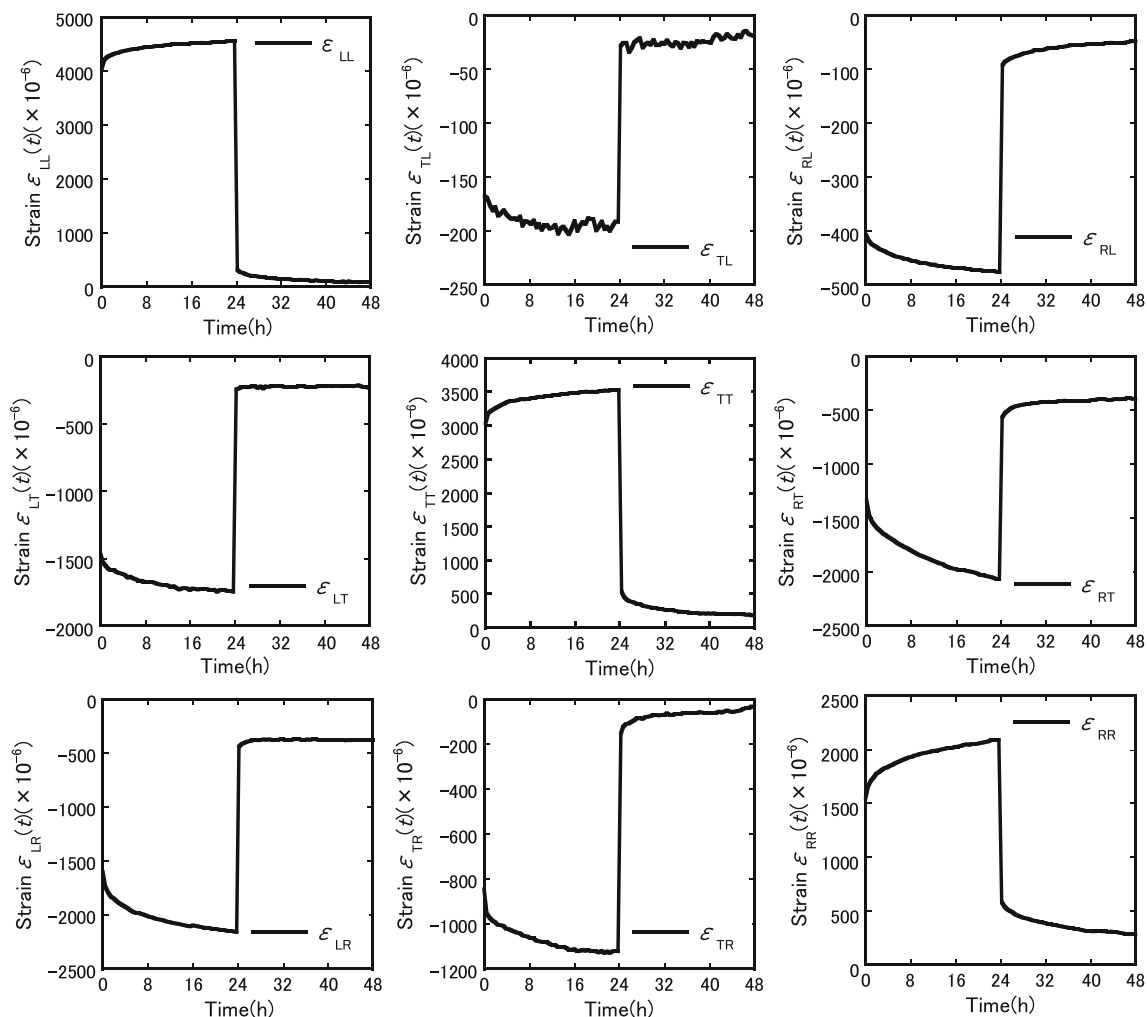


Fig. 2 Typical creep and creep-recovery curves. The first subscript in ε_{ij} represents the load direction and the second one represents the strain direction

importantly, the symmetry of the non-shear viscoelastic compliance matrix was then examined.

Theory

Three orthogonal normal strains for time-independent elastic bodies are defined by the following elastic compliance:

$$\begin{bmatrix} \varepsilon_L \\ \varepsilon_T \\ \varepsilon_R \end{bmatrix} = \begin{bmatrix} S_{LL} & S_{LT} & S_{LR} \\ S_{TL} & S_{TT} & S_{TR} \\ S_{RL} & S_{RT} & S_{RR} \end{bmatrix} \begin{bmatrix} \sigma_L \\ \sigma_T \\ \sigma_R \end{bmatrix} \\ = \begin{bmatrix} \frac{1}{E_L} & -\frac{\nu_{TL}}{E_T} & -\frac{\nu_{RL}}{E_R} \\ -\frac{\nu_{TL}}{E_L} & \frac{1}{E_T} & -\frac{\nu_{TR}}{E_R} \\ -\frac{\nu_{RL}}{E_L} & -\frac{\nu_{TR}}{E_T} & \frac{1}{E_R} \end{bmatrix} \begin{bmatrix} \sigma_L \\ \sigma_T \\ \sigma_R \end{bmatrix} \quad (3)$$

where $S_{ij}(t)$ ($i, j = L, T, R$) is the elastic compliance; ε_i ($i = L, T, R$) is normal strain when i refers to the direction of vector; σ_i is normal stress; and E_i is Young’s modulus, respectively.

When a viscoelastic material such as wood is put under a time-dependent load condition, the resulting normal strains can be expressed by the following equation:

$$\begin{bmatrix} \varepsilon_L(t) \\ \varepsilon_T(t) \\ \varepsilon_R(t) \end{bmatrix} = \begin{bmatrix} S_{LL} & S_{LT} & S_{LR} \\ S_{TL} & S_{TT} & S_{TR} \\ S_{RL} & S_{RT} & S_{RR} \end{bmatrix} \begin{bmatrix} \sigma_L \\ \sigma_T \\ \sigma_R \end{bmatrix} \\ + \begin{bmatrix} Q_{LL}(t) & Q_{LT}(t) & Q_{LR}(t) \\ Q_{TL}(t) & Q_{TT}(t) & Q_{TR}(t) \\ Q_{RL}(t) & Q_{RT}(t) & Q_{RR}(t) \end{bmatrix} \begin{bmatrix} \sigma_L \\ \sigma_T \\ \sigma_R \end{bmatrix} \quad (4)$$

where $Q_{ij}(t)$ ($i, j = L, T, R$) is the viscoelastic compliance. The first square matrix in Eq. 4 is derived from the instantaneous elastic strain, and the second one is from the delayed elastic strain and the permanent strain.

The uniaxial normal stress in i direction, σ_i , generates the stress state with $\sigma_j = \sigma_k = 0$ ($i, j, k = L, T, R; i \neq j, i \neq k$). Thus, $Q_{ii}(t)$ can be expressed as follows [28]:

$$Q_{ii}(t) = \frac{\varepsilon_i(t)}{\sigma_i} - \frac{1}{E_i} \quad (5)$$

And, $Q_{ji}(t)$ and $Q_{ki}(t)$ can be expressed as follows:

$$Q_{ji}(t) = \frac{\varepsilon_j(t)}{\sigma_i} + \frac{\nu_{ij}}{E_i} \quad (6)$$

$$Q_{ki}(t) = \frac{\varepsilon_k(t)}{\sigma_i} + \frac{\nu_{ik}}{E_i} \quad (7)$$

Materials and methods

Materials

The samples were prepared from an air-seasoning log of a 150-year-old Japanese cypress (*Chamaecyparis obtusa*

Endl.), grown in Nagano Prefecture in Japan. The diameter of a log was 41 cm. Wood was obtained from the outer growth rings (at least 20 rings from the center of the tree) of a log. Figure 1 shows an overview of tensile test specimens. The specimens were grouped into the following three types. All the specimens were derived from neighboring portions of a log.

1. L-specimen, the external dimensions were 300 (L) × 18 (T) × 18 (R) mm. A tapered shape with a central cross section of 12 mm × 12 mm and a parallel portion of about 40 mm along the fiber was formed on the LT and LR planes. Tabs made of a hardwood were attached to the grip sections on both ends of the specimen for reinforcement. E_L , σ_L , ν_{LT} , ν_{LR} , $\nu_{LT}(t)$, and $\nu_{LR}(t)$ were measured. The number of specimens was nine.
2. T-specimen, the dimensions were 250 (T) × 20 (L) × 20 (R) mm. The length of grip section was 70 mm. E_T , σ_T , ν_{TL} , ν_{TR} , $\nu_{TL}(t)$, and $\nu_{TR}(t)$ were measured. The number of specimens was eleven.
3. R-specimen, the dimensions were 120 (R) × 20 (L) × 20 (T) mm. The length of grip section was 30 mm. E_R , σ_R , ν_{RL} , ν_{RT} , $\nu_{RL}(t)$, and $\nu_{RT}(t)$ were measured. The number of specimens was ten.

Specimens were conditioned at a constant temperature of 25 °C and relative humidity of 55 % over a period of 6 months to reach an equilibrium moisture content. The density and equilibrium moisture content of specimens were $482 \pm 16 \text{ kg/m}^3$ and $9.7 \pm 0.3 \%$, respectively. The average width of annual ring was 0.9 mm.

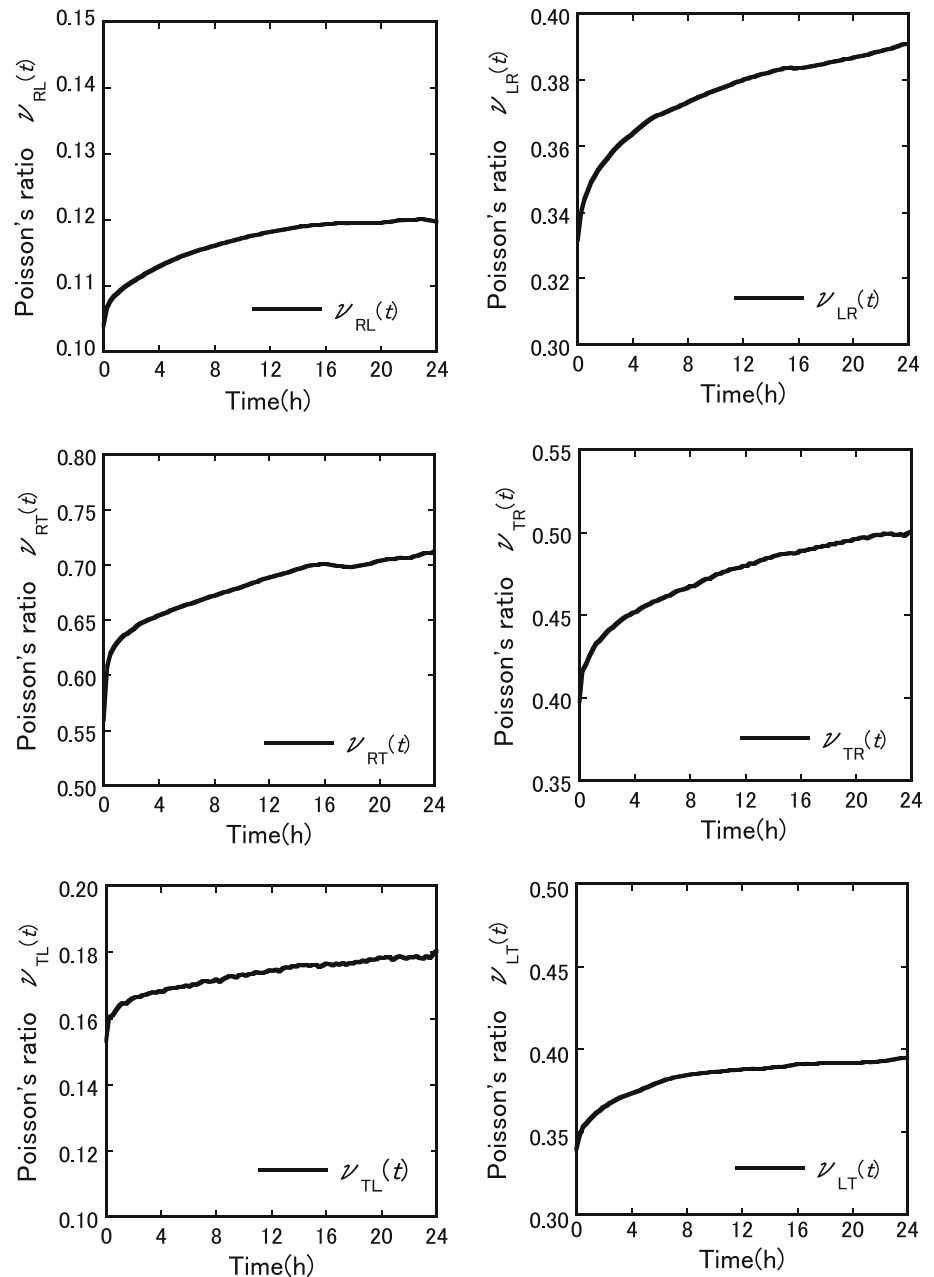
Tensile creep test

For the tensile test, a servo-controlled fatigue-testing machine (Shimadzu Servopulser EHF-ED10/TD1-20L) was used. We were able to simultaneously control both the uniaxial load and the torque using this machine, and we confirmed that all samples could be held without the possibility of twisting. Biaxial strain gauges (gauge length, 2 mm; Tokyo Sokki Kenkyujo, FCA-2-11) were pasted onto the central regions of four planes of the specimen to measure the longitudinal strain and transverse strains serially.

Beforehand, a static tensile test was conducted to measure the tensile strength. More than six specimens were used for each type of specimen.

A 24-h tensile creep test was conducted. 42, 1.5 and 2.5 MPa, which correspond to the 30 % of tensile strength in the L, T and R directions, respectively, were applied to the specimen. Thereafter, the load was removed immediately and maintained at 0 N until all strains became almost constant; this comprised the creep-recovery test. The

Fig. 3 Typical progression of viscoelastic Poisson's ratios measured during creep



temperature (25 °C) and humidity (55 %RH) were kept constant during both tests.

Results and discussion

Variations in strain

Figure 2 shows the typical changes in longitudinal and transverse strains in the L, T, and R directions of stress during creep and creep recovery. The first subscript in ε_{ij} ($i, j = L, T, R$) represents the load direction and the second represents the strain direction. Each strain is the

average value for the opposite planes. The load was removed 24 h after the beginning of the creep test. The variations in the transverse strain were similar to those in the longitudinal strain, in all directions of tensile stress. That is, during creep, the absolute value of transverse strain continued to increase with the gradual reduction in the increase rate; immediately after the removal of the load, rapid recovery occurred, after which it continued to recover slowly, in most cases, tending to converge toward a constant value.

In general, wood shows linear viscoelastic behavior in the range of bending loads up to 30–35 % of the strength. In tensile loads, this occurs up to about 50 % of the

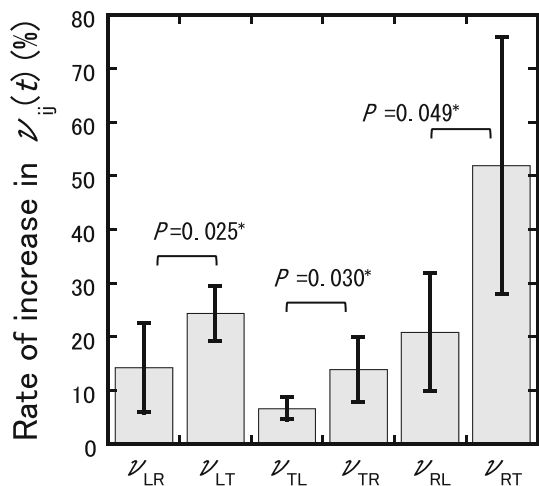


Fig. 4 Rate of increase in the viscoelastic Poisson’s ratio from the beginning of creep to after 24 h of creep. Comparison between two cases with the same loading direction. Error bars standard deviations. Asterisk significant difference (*t* test) at $p < 0.05$

strength [29]. Because the current study employed stress level of 30 % of tensile strength, the behavior observed can be assumed to lie within the linear viscoelastic range.

Variations in the viscoelastic Poisson’s ratio

Figure 3 shows the typical changes in the viscoelastic Poisson’s ratio during creep. All six viscoelastic Poisson’s ratios showed abrupt increases in the early stage. This was due to the greater increase in the absolute value of transverse strain than in the longitudinal strain during initial creep. They subsequently continued increasing gradually.

Figure 4 shows the rate of increase in the viscoelastic Poisson’s ratio from the beginning of creep to 24 h later. Comparing cases with the same loading direction, the following relationships were found ($p < 0.05$, *t* test): $\nu_{LR}(t) < \nu_{LT}(t)$, $\nu_{TL}(t) < \nu_{TR}(t)$, and $\nu_{RL}(t) < \nu_{RT}(t)$. In other words, the transverse strain increased most easily in

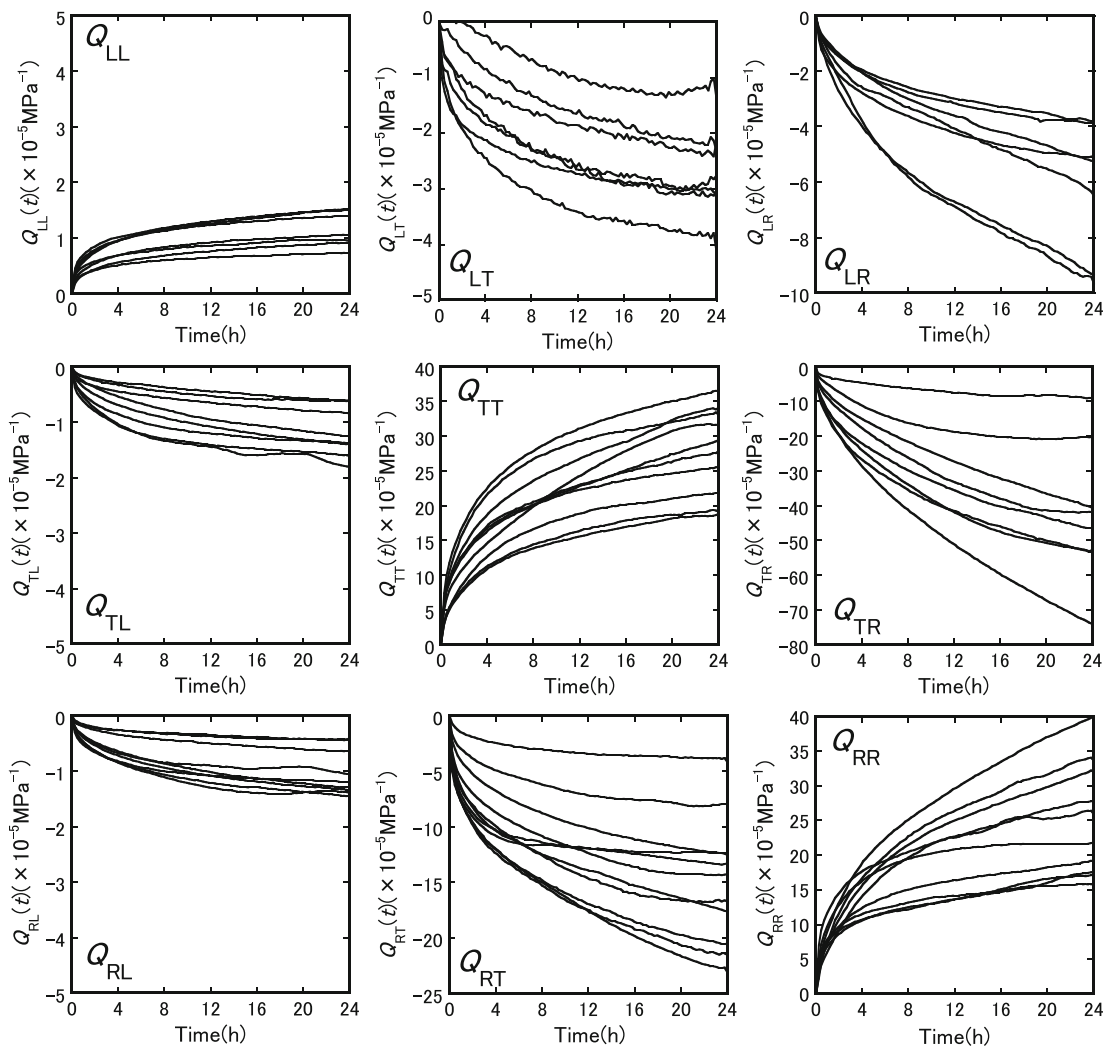


Fig. 5 Progression of the viscoelastic compliance $Q_{ij}(t)$ measured during creep. $Q_{ij}(t)$ is defined in Eq. 4

the T direction, followed by R and L, in that order ($T > R > L$). The most likely apparent reason for this is that the tracheids that lie in the L direction and the ray parenchyma cells that lie in the R direction prevent transverse strain from increasing with time.

Variations in viscoelastic compliance

Figure 5 shows the changes in viscoelastic compliance during creep. The first subscript in $Q_{ij}(t)$ indicates the strain direction, and the second one indicates the stress direction. E_i and ν_{ij} measurements were performed immediately after beginning the creep test. The diagonal elements ($i = j$) tended to increase logarithmically and the off-diagonal elements ($i \neq j$) tended to decrease logarithmically. Also, when the strain or stress was in the L direction, the values were an order of magnitude less than in the other directions.

$Q_{ij}(t)$ is approximated using the logarithm of time as $Q_{ij}(t) = a \log t + b$ (8)

where a and b are constants. Table 1 lists mean values for a and b .

Symmetry of the three-dimensional compliance matrix

In this study, the elastic compliance and viscoelastic compliance are linearly added to express strain during creep (Eq. 4). It is vital to examine whether the reciprocal compliance condition is satisfied in three orthogonal planes of wood, because this is necessary for discussing the linearity of the orthotropic viscoelasticity of wood. Before investigating the viscoelastic compliance matrix for symmetry, let us examine whether the non-shear elastic compliance matrix is symmetric.

Table 1 Mean values for a and b in Eq. 8

$Q_{ij}(t)$ (10^{-5}MPa^{-1})	n	a [$10^{-5}\text{MPa}^{-1}(\log h)^{-1}$]		b (10^{-5}MPa^{-1})	
		Average	SD	Average	SD
$Q_{LL}(t)$	9	0.45	0.13	0.56	0.14
$Q_{TL}(t)$	9	-0.53	0.19	-0.40	0.21
$Q_{RL}(t)$	9	-0.45	0.19	-0.38	0.16
$Q_{TT}(t)$	11	11.67	2.85	10.28	2.76
$Q_{RT}(t)$	11	-6.40	2.21	-6.50	1.72
$Q_{LT}(t)$	7	-1.23	0.26	-0.93	0.63
$Q_{RR}(t)$	10	10.70	5.41	9.04	1.77
$Q_{TR}(t)$	10	-21.56	10.40	-9.78	4.77
$Q_{LR}(t)$	7	-3.07	1.31	-1.35	0.36

$Q_{ij}(t)$ is defined in Eq. 4

n number of specimens, SD standard deviation

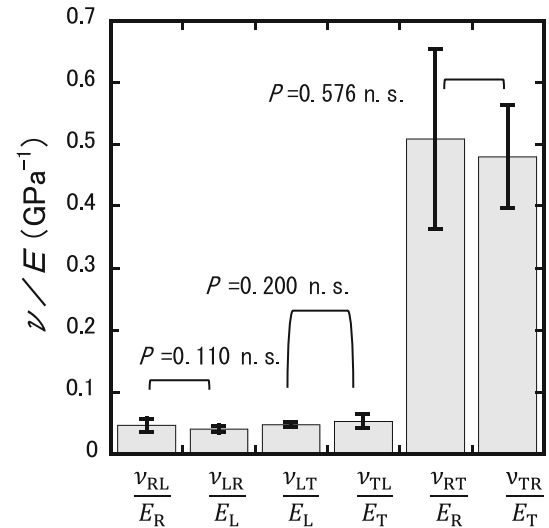


Fig. 6 Comparison of elastic compliance S_{ij} and S_{ji} . S_{ij} is defined in Eq. 3. Error bars standard deviations. *ns* non-significant difference (t test) at $p > 0.05$

Takemura [30] analyzed Hearmon’s data [31] and concluded that the elastic compliance matrix is symmetric ($S_{ij} = S_{ji}$). However, Sliker et al. [14] disagreed, reporting that while symmetry holds for S_{TR} and S_{RT} , it does not hold for the pairs S_{LR} and S_{RL} , and S_{LT} and S_{TL} . Figure 6 shows the results of an investigation of the symmetry of elastic compliance in the present study. No significant difference was found here for any of the compliance pairs ($p > 0.05$, t test). Consequently, asymmetry of three-dimensional elastic compliance matrix for Japanese cypress was not recognized in this study. The loading rate has a great influence on the measurement of Poisson’s ratio [14]; in the present study, the target load was reached in 5 s, a relatively high loading rate. Conversely, Sliker et al. measured Poisson’s ratio in static tests (strain rate in the L direction: $13\text{--}294 \times 10^{-6}/\text{min}$). It is possible that the difference in loading rates is the reason for the disparity between the finding of Sliker et al. of no symmetry and the finding in the present study.

Figure 7 shows the hourly averages of all the specimens for the off-diagonal elements in the viscoelastic compliance matrix. The figure includes $Q_{ji}(t)$, the compliance with the subscripts reversed from $Q_{ij}(t)$, to examine the symmetry of the matrix. As mentioned above, all the absolute values of the viscoelastic compliance tended to increase logarithmically. Since the error bars showing standard deviations have almost no overlap, as can be seen in the figure, a significant difference between $Q_{ij}(t)$ and $Q_{ji}(t)$ appears to exist. In view of these findings, the three-dimensional viscoelastic compliance matrix of wood is concluded to be asymmetric.

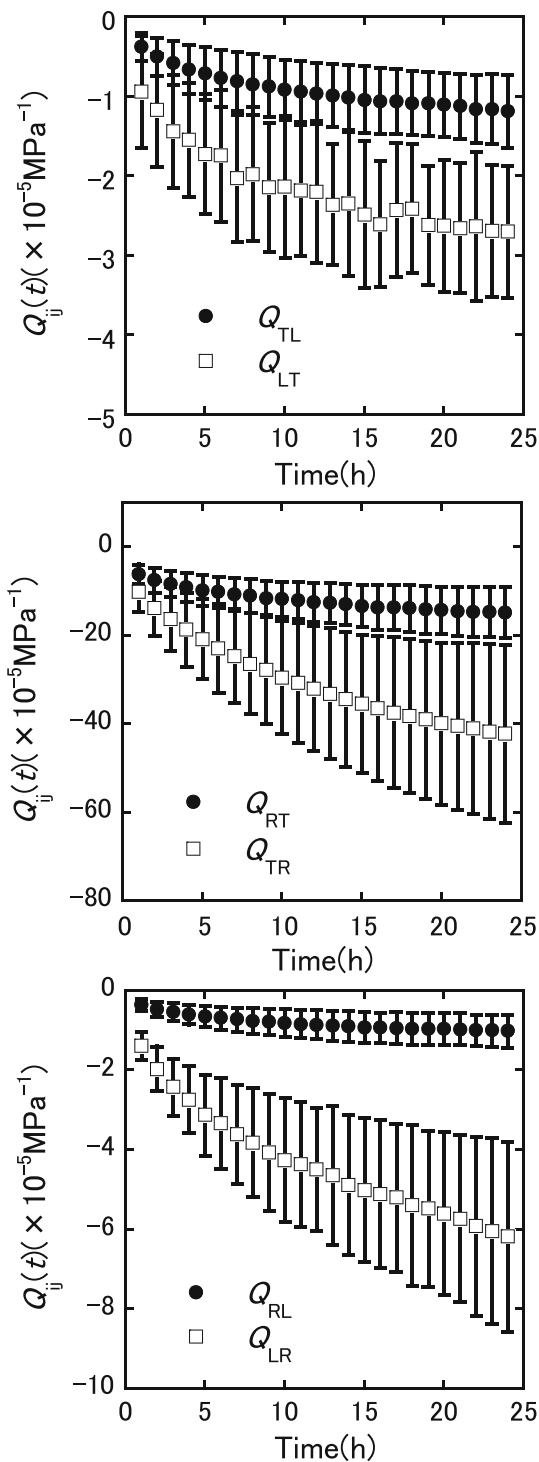


Fig. 7 Hourly averages of all the specimens for the off-diagonal elements in the non-shear viscoelastic compliance matrix, measured during creep. Comparison of $Q_{ij}(t)$ and $Q_{ji}(t)$. $Q_{ij}(t)$ is defined in Eq. 4. Error bars standard deviations

Conclusions

With the aim of understanding the viscoelasticity of wood three-dimensionally, matched samples of Japanese cypress

were loaded in uniaxial tensile creep tests in the L, T, and R directions. The longitudinal and transverse strains were measured for each type of specimen. The viscoelastic Poisson’s ratio and the viscoelastic compliance were successively determined during creep. The principal results are as follows:

1. The changes in the transverse strains showed the same tendencies as those in the longitudinal strain, in all directions of loading; specifically, the absolute value of transverse strain increased during creep, although the rate of increase in the absolute value tended to gradually decrease. Immediately after the removal of the load, transverse strain recovered sharply; subsequently, it recovered more gradually.
2. All the viscoelastic Poisson’s ratios and the diagonal elements in the non-shear viscoelastic compliance matrix increased logarithmically during creep. Conversely, the off-diagonal elements in the non-shear viscoelastic compliance matrix decreased logarithmically during creep.
3. The reciprocal elastic compliance condition for orthotropy of wood was satisfied in three dimensions.
4. The reciprocal viscoelastic compliance condition was not satisfied in any of the planes.

Extending the laws of viscoelasticity from one dimension to three dimensions allows the orthotropic viscoelasticity of wood to be expressed in a more detailed and systematic manner. This will lead to more rational designs of wood and wood-based materials as anisotropic materials.

References

1. Farruggia F, Perré P (2000) Microscopic tensile tests in the transverse plane of earlywood and latewood parts of spruce. *Wood Sci Technol* 34:65–82
2. Sinn G, Reiterer A, Stanzl-Tschegg SE, Tschegg EK (2001) Determination of strains of thin wood samples using videoextensometry. *Holz als Roh-und Werkst* 59:177–182
3. Jeong GY, Hindman DP (2010) Modeling differently oriented loblolly pine strands incorporating variation of intraring properties using a stochastic finite element method. *Wood Fiber Sci* 42:51–61
4. Ling H, Samarasinghe S, Kulasiri GD (2009) Modelling variability in full-field displacement profiles and Poisson ratio of wood in compression using stochastic neural networks. *Silva Fenn* 43:871–887
5. Dahl KB, Malo KA (2009) Planar strain measurements on wood specimens. *Exp Mech* 49:575–586
6. Yamamoto H, Kojima Y (2002) Properties of cell wall constituents in relation to longitudinal elasticity of wood. Part 1. Formulation of the longitudinal elasticity of an isolated wood fiber. *Wood Sci Technol* 36:55–74
7. Nakamura K, Wada M, Kuga S, Okano T (2004) Poisson’s ratio of cellulose I_{β} and cellulose II. *J Polym Sci Part B Polym Phys* 42:1206–1211

8. Marklund E, Varna J (2009) Modeling the effect of helical fiber structure on wood fiber composite elastic properties. *Appl Compos Mater* 16:245–262
9. Qing H, Mishnaevsky L Jr (2010) 3D multiscale micromechanical model of wood: from annual rings to microfibrils. *Int J Solids Struct* 47:1253–1267
10. Ozyhar T, Hering S, Niemz P (2012) Moisture-dependent elastic and strength anisotropy of European beech wood in tension. *J Mater Sci* 47:6141–6150
11. Hering S, Keunecke D, Niemz P (2012) Moisture-dependent orthotropic elasticity of beech wood. *Wood Sci Technol* 46:927–938
12. Reiterer A, Stanzl-Tschegg SE (2001) Compressive behaviour of softwood under uniaxial loading at different orientations to the grain. *Mech Mater* 33:705–715
13. Garab J, Keunecke D, Hering S, Szalai J, Niemz P (2010) Measurement of standard and off-axis elastic moduli and Poisson's ratios of spruce and yew wood in the transverse plane. *Wood Sci Technol* 44:451–464
14. Sliker A, Yu Y, Weigel T, Zhang W (1994) Orthotropic elastic constants for eastern hardwood species. *Wood Fiber Sci* 26:107–121
15. Jeong GY, Zink-Sharp A, Hindman DP (2010) Applying digital image correlation to wood strands: influence of loading rate and specimen thickness. *Holzforschung* 64:729–734
16. Yoshihara H, Tsunematsu S (2007) Elastic properties of compressed spruce with respect to its cross section obtained under various compression ratios. *For Prod J* 57(4):98–100
17. Anshari B, Guan ZW, Kitamori A, Jung K, Hassel I, Komatsu K (2011) Mechanical and moisture-dependent swelling properties of compressed Japanese cedar. *Constr Build Mater* 25:1718–1725
18. Wetzig M, Heldstab C, Tauscher T, Niemz P (2011) Determination of select mechanical properties of heat-treated beech wood (in German). *Bauphysik* 33:366–373
19. Gonçalves R, Trinca AJ, Cerri DGP (2011) Comparison of elastic constants of wood determined by ultrasonic wave propagation and static compression testing. *Wood Fiber Sci* 43:64–75
20. Kohlhauser C, Hellmich C (2012) Determination of Poisson's ratios in isotropic, transversely isotropic, and orthotropic materials by means of combined ultrasonic-mechanical testing of normal stiffnesses: application to metals and wood. *Eur J Mech A Solids* 33:82–98
21. Hilton HH, Yi S (1998) The significance of (an)isotropic viscoelastic Poisson ratio stress and time dependencies. *Int J Solids Struct* 35:3081–3095
22. Hilsenrath H (2001) Implications and constraints of time-independent Poisson ratios in linear isotropic and anisotropic viscoelasticity. *J Elast* 63:221–251
23. Sobue N, Takemura T (1979) Poisson's ratios in dynamic viscoelasticity of wood as two-dimensional materials. *Mokuzai Gakkaishi* 25:258–263
24. Schniewind AP, Barrett JD (1972) Wood as a linear orthotropic viscoelastic material. *Wood Sci Technol* 6:43–57
25. Hayashi K, Felix B, Le Govic C (1993) Wood viscoelastic compliance determination with special attention to measurement problems. *Mater Struct* 26:370–376
26. Taniguchi Y, Ando K (2010) Time dependence of Poisson's effect in wood I: the lateral strain behavior. *J Wood Sci* 56:100–106
27. Taniguchi Y, Ando K (2010) Time dependence of Poisson's effect in wood II: volume change during uniaxial tensile creep. *J Wood Sci* 56:350–354
28. Taniguchi Y, Ando K, Yamamoto H (2010) Determination of three-dimensional viscoelastic compliance in wood by tensile creep test. *J Wood Sci* 56:82–84
29. Navi P, Stanzl-Tschegg S (2009) Micromechanics of creep and relaxation of wood. A review COST Action E35 2004–2008: wood machining—micromechanics and fracture. *Holzforschung* 63:186–195
30. Takemura T (1985) Elasticity (in Japanese). In: *Wood physics*. Bun-eido, Tokyo, pp 94–115
31. Hearmon RFS (1948) The elastic constants of wood. In: *The elasticity of wood and plywood*. Forest products research special report No. 7. His Majesty's Stationery Office, London, pp 5–44